Differential Spatial Modulation Using New Index Bits

Vahid ABBASI, Mahrokh G. SHAYESTEH

Dept. of Electrical Engineering, Urmia University, Urmia 57561-15311, Iran

va.abbasi@urmia.ac.ir, m.shayesteh@urmia.ac.ir

Submitted June 19, 2023 / Accepted November 26, 2023 / Online first February 19, 2024

Abstract. *Spatial modulation (SM) has the potential to meet the requirements of 5G and beyond communication systems with features such as reduced hardware complexity and good trade-off between spectral efficiency and energy efficiency. In this study, an efficient non-square differential spatial modulation (DSM) scheme is presented in which the number of time slots is one more than the number of transmit antennas. The introduced scheme includes one empty time slot. At the other time slots, the time slots of the conventional DSM (CDSM) are used (the Gray code order (GCO) can also be used). There is one active antenna at each time slot of the proposed scheme. The index of empty time slot conveys information. Thus, in comparison with CDSM (or GCO), for the same number of transmit antennas, the introduced scheme has more energy-free bits (index bits). It is free of pilot overhead, channel estimation complexity, and potential channel state information (CSI) estimation errors. Further, a detector with no error propagation is presented. Analytical expressions for the bit error rate (BER) are derived at high signal-to-noise ratios (SNRs) and high SNRs per bit (SNRbs). Simulation results verify the theoretical evaluation and demonstrate the efficiency of the proposed scheme.*

Keywords

Index modulation, 5G, time index modulation, differential spatial modulation (DSM), single active antenna, error propagation, diversity, signal to noise per bit (SNRb)

1. Introduction

There are many challenges to achieve the objectives of 5G and beyond communication systems [1]. Successful implementation of 5G will enable anywhere, anytime, anyhow connectivity [1]. Index modulation (IM) techniques have the potential for meeting the requirements of 5G mobile systems [2]. IM provides an attractive trade-off among different characteristics of communication systems [3]. IMs are capable of conveying extra information by utilizing the available transmit entities, such as the indices of antennas, subcarriers, time slots, and so on [3]. IM was initially introduced by using the indices of antennas (spatial modulation (SM)) for multiple-input multiple-output (MIMO) communication systems [4]. SM utilizes antenna indices and allows for a low-cost and high-energy-efficiency system with low hardware complexity [3]. Differential SM (DSM) was introduced as a promising alternative to coherent SMs [5]. DSMs are desirable for wireless systems that have fast migration velocity [6]. In [7], a unified DSM scheme using complex-valued antenna index matrices was introduced [8]. Transmit diversity order in [7] was obtained by transmitting the same symbols on multiple antennas [8]. Therefore, a flexible rate-diversity trade-off was achieved [9]. After that, Gray code order (GCO) and intersected GCO (I-GCO) of antenna index permutations were presented in [10] to improve the performance of DSMs [11]. I-GCO exhibits higher transmit diversity order, when compared to GCO. In [10], some new bit-to-symbol mapping principles were used [12]. Conventional DSM (CDSM) ([7], [13]), GCO, and I-GCO are free of pilot overhead, channel estimation complexity, and potential channel state information (CSI) estimation errors. However, several DSMs were studied in [14], [15], [16], and [17]. There is one active antenna at each time slot of CDSM [7], [13], [10], [14–17]. Although, [14–17] do not need CSI, all of them have pilot overhead [5]. Further, they suffer from error propagation [5].

In this research, we combine CDSM (or GCO) and time-domain IM to take the advantages of both techniques. The proposed scheme includes one empty time slot and the other time slots are time slots of CDSM (or GCO). The index of the empty time slot conveys information. Therefore, compared to the CDSM (or GCO), the introduced scheme transmits additional energy-free bits, without increasing the number of transmit antennas. In this way, we overcome the limitation on the number of time slots of CDSM (or GCO) (which is equal to the number of transmit antennas). The proposed DSM does not require any pilot overhead and CSI. Further, we introduce a detector that avoids error propagation. Theoretical analysis and simulation results show that at high signal-to-noise ratios (SNRs) and signal-to-noise ratios per bit (SNRbs), the presented scheme outperforms CDSM and GCO.

Notations: Small letters, bold letters, and bold capital letters designate scalars, vectors, and matrices, respectively. $\llbracket \cdot \rrbracket$ is the floor function and $\llbracket \cdot \rrbracket_2$ is equal to $\llbracket \log_2(\cdot) \rrbracket$. $\mathbf{A}(i,:)$ and $\mathbf{A}(:,i)$ show the i-th row and i-th column of ma-

DOI: 10.13164/re.2024.0173

trix $\mathbf{A}$ respectively. E(·), |·|, and diag($\mathbf{v}$) denote expectation, absolute value, and diagonal matrix with the elements of the vector $\mathbf{v}$, respectively. In $r \angle \theta$, r indicates absolute value and θ denotes angle. $(\cdot)^{\mathrm{T}}$, $\|\cdot\|_{\mathrm{F}}^2$, and tr(·) represent transpose, Frobenious norm, and trace, respectively.

2. Proposed Scheme

2.1 System Model

A MIMO system with N transmit antennas and M receive antennas is considered. The wireless channel is assumed constant over a block of length T, i.e., quasi-static Rayleigh flat fading. Moreover, the receiver and transmitter do not know CSI. The input-output relation is $\mathbf{Y}_t = \mathbf{X}_t \mathbf{H}_t + \mathbf{N}_t$, where the transmitted and received signal at the t-th block are $T \times N$ matrix $\mathbf{X}_t$ and $T \times M$ matrix $\mathbf{Y}_t$, respectively. The elements of the $N \times M$ complex channel matrix $\mathbf{H}_t$ and $T \times M$ complex noise matrix $\mathbf{N}_t$ are zero-mean, independent and identically distributed (i.i.d) Gaussian random variables with unit variance.

We design the proposed scheme by employing the structure of CDSM or GCO. To this end, we first review CDSM briefly.

2.2 CDSM System

In CDSM, only one transmit antenna is activated at each time slot, and information bits are conveyed by the square antenna matrix (AM) index (since $T = N$, block matrix is $N \times N$) and the constellation diagram [17]. The input vector $\mathbf{s}_t = [s_1,\ldots,s_N]$ is mapped into the input AM $\mathbf{A}_t$ as $\mathbf{S}_t = \mathbf{A}_t \,\mathrm{diag}(\mathbf{s}_t)$, where $s_1,\ldots,s_N$ are drawn from the phase shift keying (PSK) constellation. The transmitted signal matrix at the t-th block has the form of $\mathbf{X}_t = \mathbf{S}_t \mathbf{X}_{t-1}$ [17]. The non-coherent maximum likelihood (ML) detector is expressed as

$$\hat{\mathbf{S}}_t = \arg\min_{\tilde{\mathbf{S}}_t \in \mathbb{S}} \| \mathbf{Y}_t - \tilde{\mathbf{S}}_t \mathbf{Y}_{t-1} \|_{\mathrm{F}}^2 \qquad (1)$$

where $\mathbb{S}$ is the set of all possible matrices [13]. In the non-coherent ML detector, all members of $\mathbb{S}$ are tested one by one [18]. Assuming $\mathbf{H}_t = \mathbf{H}_{t-1}$, we have

$$\mathbf{Y}_t - \tilde{\mathbf{S}}_t \mathbf{Y}_{t-1} = (\mathbf{S}_t - \tilde{\mathbf{S}}_t)\mathbf{X}_{t-1}\mathbf{H}_t + (\mathbf{N}_t - \tilde{\mathbf{S}}_t \mathbf{N}_{t-1}) . \qquad (2)$$

It is observed that the effective noise power is twice that of the coherent SM, resulting in 3-dB SNR penalty. If the minimum rank of $\Delta\mathbf{S}_t = \mathbf{S}_t - \tilde{\mathbf{S}}_t$ for $\Delta\mathbf{S}_t \neq \mathbf{0}$ is d_{x}, the diversity order of the CDSM would be Md_{x}.

2.3 Proposed Scheme

We explain the method of constructing the proposed scheme using the structure of CDSM. The method of constructing the proposed code using GCO is similar.

The proposed scheme, $\mathbf{X}_t^{\mathrm{P}}$, consists of one empty time slot (the o_t-th time slot) and N time slots of an CDSM ($\mathbf{X}_t$), so, $T = N + 1$ (in CDSM, $T = N$). In $\mathbf{X}_t^{\mathrm{P}}$, the index of empty time slot conveys information, and no data transmission occurs in that time slot. The information of the time slots $N + 2 - o_t,\ldots,N$ of $\mathbf{X}_t$ is sent at the time slots $1,\ldots,o_t - 1$ of $\mathbf{X}_t^{\mathrm{P}}$, respectively. Similarly, the information of the time slots 1, …, $N + 1 - o_t$ of $\mathbf{X}_t$ is transmitted at the time slots $o_t + 1,\ldots,N + 1$ of $\mathbf{X}_t^{\mathrm{P}}$. The proposed $\mathbf{X}_t^{\mathrm{P}}$ can be expressed in terms of $\mathbf{X}_t$ as

$$\mathbf{X}_t^{\mathrm{P}} = c_t \mathbf{C}_t \mathbf{X}_t = c_t \mathbf{C}_t \mathbf{S}_t \mathbf{X}_{t-1} = c_t \mathbf{C}_t \mathbf{A}_t \,\mathrm{diag}(\mathbf{s}_t)\mathbf{X}_{t-1} \qquad (3)$$

where $\mathbf{C}_t$ and c_t are $(N + 1) \times N$ matrix and complex coefficient, respectively. $\mathbf{C}_t$ and c_t depend on the index of empty time slot o_t. The relationship between $\mathbf{C}_t$ and o_t can be written as follows:

$$\begin{cases} \mathbf{C}_t(o_t,:) = \mathbf{0}_{1\times N}, & \\ \mathbf{C}_t(o_t + i,:) = \mathbf{I}_N(i,:), & o_t + i \le N + 1,\ i \ge 1, \\ \mathbf{C}_t(o_t - i,:) = \mathbf{I}_N(N + 1 - i,:), & o_t - i < N,\quad i \ge 1 \end{cases} \qquad (4)$$

where $\mathbf{I}_N$ is the $N \times N$ identity matrix. As an example, for $N = 3$, and $o_t = 1$, $o_t = 2$, $o_t = 3$, $o_t = 4$, the transmit signal matrices are provided in Tab. 1.

It can be shown that $\mathbf{C}_t^{\mathrm{T}} \mathbf{C}_t = \mathbf{I}_N$. Since $\mathbf{X}_t^{\mathrm{P}}$ has $T = N + 1$ time slots (resulting in $N + 1$ choices for o_t), there are $\llbracket N + 1 \rrbracket_2$ new index bits compared to the utilized CDSM ($\mathbf{X}_t$). Consequently, the number of bits of $\mathbf{X}_t^{\mathrm{P}}$ is $B_{\mathrm{X^P}} = B_{\mathrm{X}} + \llbracket N + 1 \rrbracket_2$, where B_{X} is the number of bits of the utilized CDSM ($\mathbf{X}_t$). The throughput (represented as bit per channel use (bpcu)) of $\mathbf{X}_t^{\mathrm{P}}$ in (3) is $\bar{B}_{\mathrm{X^P}} = (B_{\mathrm{X}} + \llbracket N + 1 \rrbracket_2) / (N + 1)$. The received signal at the receiver is given by $\mathbf{Y}_t = \mathbf{X}_t^{\mathrm{P}} \mathbf{H}_t + \mathbf{N}_t$.

	$\mathbf{C}_t$	$\mathbf{X}_t^{\mathrm{P}} = c_t \mathbf{C}_t \mathbf{X}_t$
$o_t = 1$	$\begin{bmatrix} 0 & 0 & 0 \\ 1 & 0 & 0 \\ 0 & 1 & 0 \\ 0 & 0 & 1 \end{bmatrix}$	$c_t \begin{bmatrix} 0 & 0 & 0 \\ \mathbf{X}_t(1,:) \\ \mathbf{X}_t(2,:) \\ \mathbf{X}_t(3,:) \end{bmatrix}$
$o_t = 2$	$\begin{bmatrix} 0 & 0 & 1 \\ 0 & 0 & 0 \\ 1 & 0 & 0 \\ 0 & 1 & 0 \end{bmatrix}$	$c_t \begin{bmatrix} \mathbf{X}_t(3,:) \\ 0 & 0 & 0 \\ \mathbf{X}_t(1,:) \\ \mathbf{X}_t(2,:) \end{bmatrix}$
$o_t = 3$	$\begin{bmatrix} 0 & 1 & 0 \\ 0 & 0 & 1 \\ 0 & 0 & 0 \\ 1 & 0 & 0 \end{bmatrix}$	$c_t \begin{bmatrix} \mathbf{X}_t(2,:) \\ \mathbf{X}_t(3,:) \\ 0 & 0 & 0 \\ \mathbf{X}_t(1,:) \end{bmatrix}$
$o_t = 4$	$\begin{bmatrix} 1 & 0 & 0 \\ 0 & 1 & 0 \\ 0 & 0 & 1 \\ 0 & 0 & 0 \end{bmatrix}$	$c_t \begin{bmatrix} \mathbf{X}_t(1,:) \\ \mathbf{X}_t(2,:) \\ \mathbf{X}_t(3,:) \\ 0 & 0 & 0 \end{bmatrix}$

Tab. 1. Transmit signal matrices of the proposed $\mathbf{X}_t^{\mathrm{P}}$ for $N = 3$, and $o_t = 1$, $o_t = 2$, $o_t = 3$, $o_t = 4$.

2.4 Proposed Detector

Noting $\mathbf{C}_{t-1}^{\mathrm{T}} c_{t-1}^{-1} c_{t-1} \mathbf{C}_{t-1} = \mathbf{I}_N$ and $\mathbf{X}_{t-1}^{\mathrm{P}} = c_{t-1} \mathbf{C}_{t-1} \mathbf{X}_{t-1}$, we can establish the relationship

$$\mathbf{X}_{t-1} = \mathbf{C}_{t-1}^{\mathrm{T}} c_{t-1}^{-1} c_{t-1} \mathbf{C}_{t-1} \mathbf{X}_{t-1} = \mathbf{C}_{t-1}^{\mathrm{T}} c_{t-1}^{-1} \mathbf{X}_{t-1}^{\mathrm{P}}. \quad (5)$$

Subsequently, considering $\mathbf{X}_t^{\mathrm{P}} = c_t \mathbf{C}_t \mathbf{S}_t \mathbf{X}_{t-1}$, we obtain $\mathbf{X}_t^{\mathrm{P}} = c_t \mathbf{C}_t \mathbf{S}_t \mathbf{C}_{t-1}^{\mathrm{T}} c_{t-1}^{-1} \mathbf{X}_{t-1}^{\mathrm{P}}$. Since $\mathbf{H}_t = \mathbf{H}_{t-1}$ we find that $\mathbf{X}_t^{\mathrm{P}} \mathbf{H}_t = c_t \mathbf{C}_t \mathbf{S}_t \mathbf{C}_{t-1}^{\mathrm{T}} c_{t-1}^{-1} \mathbf{X}_{t-1}^{\mathrm{P}} \mathbf{H}_{t-1}$ and

$$\mathbf{Y}_t - c_t \mathbf{C}_t \mathbf{S}_t \mathbf{C}_{t-1}^{\mathrm{T}} c_{t-1}^{-1} \mathbf{Y}_{t-1} = \mathbf{N}_t - c_t \mathbf{C}_t \mathbf{S}_t \mathbf{C}_{t-1}^{\mathrm{T}} c_{t-1}^{-1} \mathbf{N}_{t-1}. \quad (6)$$

Hence, we propose the following detector

$$\hat{o}_t, \hat{\mathbf{S}}_t = \underset{\tilde{o}_t, \tilde{o}_{t-1}, \tilde{\mathbf{S}}_t}{\arg\min} \| \mathbf{Y}_t - \tilde{c}_t \tilde{\mathbf{C}}_t \tilde{\mathbf{S}}_t \tilde{\mathbf{C}}_{t-1}^{\mathrm{T}} \tilde{c}_{t-1}^{-1} \mathbf{Y}_{t-1} \|_{\mathrm{F}}^2. \quad (7)$$

In the above detector, we consider all possible cases of $\tilde{o}_{t-1}$, and we do not use $\hat{o}_{t-1}$ which is detected in the $(t-1)$-th received block. This design ensures that the error in the $(t-1)$-th block detection does not affect the t-th block detection. Therefore, the proposed detector, (7), avoids error propagation.

Since $\mathbf{H}_t = \mathbf{H}_{t-1}$, the matrix in (7) can be expressed as

$$\begin{aligned} &\mathbf{Y}_t - \tilde{c}_t \tilde{\mathbf{C}}_t \tilde{\mathbf{S}}_t \tilde{\mathbf{C}}_{t-1}^{\mathrm{T}} \tilde{c}_{t-1}^{-1} \mathbf{Y}_{t-1} \\ &\quad = (\underbrace{c_t \mathbf{C}_t \mathbf{S}_t}_{\mathbf{F}_t} - \underbrace{\tilde{c}_t \tilde{\mathbf{C}}_t \tilde{\mathbf{S}}_t \tilde{\mathbf{C}}_{t-1}^{\mathrm{T}} \tilde{c}_{t-1}^{-1} c_{t-1} \mathbf{C}_{t-1}}_{\mathbf{Q}_t}) \mathbf{X}_{t-1} \mathbf{H}_t \\ &\quad + (\underbrace{\mathbf{N}_t - \tilde{c}_t \tilde{\mathbf{C}}_t \tilde{\mathbf{S}}_t \tilde{\mathbf{C}}_{t-1}^{\mathrm{T}} \tilde{c}_{t-1}^{-1} \mathbf{N}_{t-1}}_{\mathbf{N}_t^{\mathrm{D}}}). \end{aligned} \quad (8)$$

3. Analytical Evaluation

3.1 Diversity Order of $\mathbf{X}_t^{\mathrm{P}}$

We assume that o'_{t-1}, $\hat{o}_t$, and $\hat{\mathbf{S}}_t$ minimize the metric in (7). As a result, both $\hat{o}_t$ and $\hat{\mathbf{S}}_t$ are detected (it is worth noting that the values of o'_{t-1} and $\hat{o}_{t-1}$ may differ). In the analysis, we define two complementary events O and Ø as $[o'_{t-1}, \hat{o}_t] = [o_{t-1}, o_t]$ and $[o'_{t-1}, \hat{o}_t] \neq [o_{t-1}, o_t]$ respectively. These events help us in finding the error probabilities and diversity order. If we denote the error probability in detecting X^{P} as $\mathrm{P}_{\mathrm{X}^{\mathrm{P}}}$, we can express it as the combination of two conditional probabilities as $\mathrm{P}_{\mathrm{X}^{\mathrm{P}}} = \mathrm{P}_{\mathrm{O}} \mathrm{P}_{\mathrm{X}^{\mathrm{P}}|\mathrm{O}} + \mathrm{P}_{\text{Ø}} \mathrm{P}_{\mathrm{X}^{\mathrm{P}}|\text{Ø}}$, where $\mathrm{P}_{\mathrm{X}^{\mathrm{P}}|\mathrm{O}}$ and $\mathrm{P}_{\mathrm{X}^{\mathrm{P}}|\text{Ø}}$ represent the error probabilities in detecting X^{P} under the conditions O and Ø, respectively. We define $Md_{\text{Ø}}$ as the diversity order of Ø. At high SNRs, $\mathrm{P}_{\text{Ø}}$ and $\mathrm{P}_{\mathrm{X}^{\mathrm{P}}|\mathrm{O}}$ are proportional to $SNR^{-d_{\text{Ø}}M}$ and $SNR^{-d_{\mathrm{X}}M}$ [19], respectively. Additionally, considering $\mathrm{P}_{\mathrm{O}} = 1 - \mathrm{P}_{\text{Ø}}$, we have $\mathrm{P}_{\mathrm{X}^{\mathrm{P}}} = \mathrm{P}_{\mathrm{X}^{\mathrm{P}}|\mathrm{O}} + \mathrm{P}_{\text{Ø}} (\mathrm{P}_{\mathrm{X}^{\mathrm{P}}|\text{Ø}} - \mathrm{P}_{\mathrm{X}^{\mathrm{P}}|\mathrm{O}})$. As a result, if $Md_{\text{Ø}} \geq Md_{\mathrm{X}}$, the diversity order of $\mathbf{X}_t^{\mathrm{P}}$ will be Md_{X}. Furthermore, if $Md_{\text{Ø}} > Md_{\mathrm{X}}$, at high SNRs we have $\mathrm{P}_{\mathrm{X}^{\mathrm{P}}} = \mathrm{P}_{\mathrm{X}^{\mathrm{P}}|\mathrm{O}}$. In the following, we will investigate $\mathrm{P}_{\mathrm{X}^{\mathrm{P}}|\mathrm{O}}$ and the diversity order of Ø.

3.2 Conditional BER

In this sub-section we focus on the conditional BER $\mathrm{P}_{\mathrm{X}^{\mathrm{P}}|\mathrm{O}}$. Given that $\hat{o}_t$, o'_{t-1}, and $\hat{\mathbf{S}}_t$ minimize the metric in (7) (it is important to note that o'_{t-1} does not imply the detected o_{t-1}), for the event O we have $\tilde{o}_{t-1} = o_{t-1}$, $\tilde{o}_t = o_t$, which in turn results in $\tilde{\mathbf{C}}_t = \mathbf{C}_t$, $\tilde{\mathbf{C}}_{t-1} = \mathbf{C}_{t-1}$, $\tilde{c}_{t-1} = c_{t-1}$, and $\tilde{c}_t = c_t$. Therefore,

$$\begin{aligned} &\mathbf{Y}_t - \tilde{c}_t \tilde{\mathbf{C}}_t \tilde{\mathbf{S}}_t \tilde{\mathbf{C}}_{t-1}^{\mathrm{T}} \tilde{c}_{t-1}^{-1} \mathbf{Y}_{t-1} \\ &\quad = c_t \mathbf{C}_t (\mathbf{S}_t - \tilde{\mathbf{S}}_t) \mathbf{X}_{t-1} \mathbf{H}_t \\ &\quad + (\mathbf{N}_t - c_t \mathbf{C}_t \tilde{\mathbf{S}}_t \mathbf{C}_{t-1}^{\mathrm{T}} c_{t-1}^{-1} \mathbf{N}_{t-1}). \end{aligned} \quad (9)$$

Considering the structures of $\mathbf{C}_t$ and $\tilde{\mathbf{S}}_t$, it is evident that $\mathbf{C}_{t-1}^{\mathrm{T}} c_{t-1}^{-1} \mathbf{N}_{t-1}$ and $\tilde{\mathbf{S}}_t \mathbf{C}_{t-1}^{\mathrm{T}} c_{t-1}^{-1} \mathbf{N}_{t-1}$ are $N \times M$ matrices where none of their elements are zero. Consequently, $c_t \mathbf{C}_t \tilde{\mathbf{S}}_t \mathbf{C}_{t-1}^{\mathrm{T}} c_{t-1}^{-1} \mathbf{N}_{t-1}$ is an $(N+1) \times M$ matrix, and only its o_t-th row is empty. This indicates that the o_t-th row of $\mathbf{N}_t - c_t \mathbf{C}_t \tilde{\mathbf{S}}_t \mathbf{C}_{t-1}^{\mathrm{T}} c_{t-1}^{-1} \mathbf{N}_{t-1}$ contains only the noise $\mathbf{N}_t(o_t,:)$, which is independent of $\tilde{\mathbf{S}}_t$ and therefore, has no influence on the detector. Additionally, in (9), the o_t-th time slot of $c_t \mathbf{C}_t (\mathbf{S}_t - \tilde{\mathbf{S}}_t) \mathbf{X}_{t-1} \mathbf{H}_t$ is empty and does not affect the detector. As a result, the o_t-th time slot in (9) does not have an impact on the detector. Consequently, considering N effective time slots of (9) (o_t-th time slot is not effective), $\mathbf{X}_t^{\mathrm{P}}$ is equivalent to an CDSM ((9) is similar to (2)) with the effective noise power $1 + |c_t c_{t-1}^{-1}|^2$ and average signal power $|c_t|^2 \mathrm{E}_{\mathrm{X}} / N$, where $\mathrm{E}_{\mathrm{X}} = \mathrm{E}(\mathrm{tr}(\mathbf{X}_t^{\mathrm{H}} \mathbf{X}_t))$. Each of o_t and o_{t-1} can take $2^{\lfloor N+1 \rfloor_2}$ values, leading to $L = 2^{2\lfloor N+1 \rfloor_2}$ different cases for the event O. In each case $l = 1,\ldots,L$, the effective SNR of the equivalent CDSM is $\sigma_l \mathrm{E}_{\mathrm{X}} / N$, where $\sigma_l = |c_t c_{t-1}|^2 / (|c_{t-1}|^2 + |c_t|^2)$. Then, the BER of $\mathbf{X}_t^{\mathrm{P}}$ is $B_{\mathrm{X}} \mathrm{P}_{\mathrm{X}} (SNR_{\mathrm{X}} = u_l) / B_{\mathrm{X}^{\mathrm{P}}}$, where $u_l = 2 \sigma_l \mathrm{E}_{\mathrm{X}} / N$ (u_l is the SNR of the equivalent CDSM for each case). The SNR of $\mathbf{X}_t^{\mathrm{P}}$ is $u_{\mathrm{X}^{\mathrm{P}}} = \mathrm{E}_c \mathrm{E}_{\mathrm{X}} / (N+1)$, where $\mathrm{E}_c = \mathrm{E}(|c_t|^2)$ (please note that u_l and $u_{\mathrm{X}^{\mathrm{P}}}$ are not effective SNRs). Since O has L cases, we can express the conditional error probability as

$$\begin{aligned} &\mathrm{P}_{\mathrm{X}^{\mathrm{P}}|\mathrm{O}} (SNR_{\mathrm{X}^{\mathrm{P}}} = u_{\mathrm{X}^{\mathrm{P}}}) \\ &\quad = L^{-1} \sum_{l=1}^{L} (B_{\mathrm{X}} \mathrm{P}_{\mathrm{X}} (SNR_{\mathrm{X}} = u_l) / B_{\mathrm{X}^{\mathrm{P}}}). \end{aligned} \quad (10)$$

Therefore, the diversity order of X^{P} under the condition O is Md_{X}.

3.3 Diversity Order of Ø

In this sub-section, we determine the rank of the matrix $\mathbf{D}_t \mathbf{X}_{t-1}$, where $\mathbf{D}_t = \mathbf{F}_t - \mathbf{Q}_t$ (note (8)). Since the $N \times N$ matrix $\mathbf{X}_{t-1}$ is invertible (due to having one non-zero element in each row and column of $\mathbf{X}_{t-1}$), the rank of $\mathbf{D}_t \mathbf{X}_{t-1}$ is the same as that of $\mathbf{D}_t$ [20]. Therefore, we only examine the rank of $\mathbf{D}_t$ for the event Ø. From (8) we note that

$$\mathbf{D}_t = \mathbf{F}_t - \mathbf{Q}_t = c_t \mathbf{C}_t \mathbf{S}_t - \tilde{c}_t \tilde{\mathbf{C}}_t \tilde{\mathbf{S}}_t \tilde{\mathbf{C}}_{t-1}^{\mathrm{T}} \tilde{c}_{t-1}^{-1} c_{t-1} \mathbf{C}_{t-1}. \quad (11)$$

We use s_n to represent the non-zero element in the n-th column of $\mathbf{C}_t \mathbf{S}_t$. If the n-th column of $\tilde{\mathbf{C}}_t \tilde{\mathbf{S}}_t \tilde{\mathbf{C}}_{t-1}^{\mathrm{T}} \mathbf{C}_{t-1}$ contains a non-zero element, we denote it as $\tilde{s}_n$.

As per the details provided in Appendix A, if we can establish the equation

$$s_{i_1} \ldots s_{i_k} c_t^k \neq (\tilde{c}_t \, \tilde{c}_{t-1}^{-1} \, c_{t-1})^k \, \tilde{s}_{i_1} \ldots \tilde{s}_{i_k}, \quad k = 1, \ldots, d, \quad d \leq N \tag{12}$$

for all cases of Ø, all values of $s_{i_1}, \ldots, s_{i_k}, \tilde{s}_{i_1}, \ldots, \tilde{s}_{i_k}$, and all distinct values of $i_1, \ldots, i_k$ ($1 \leq i_1, \ldots, i_k \leq N$), we will have $\mathrm{rank}(\mathbf{D}_t) \geq d$, $\mathrm{rank}(\mathbf{D}_t \mathbf{X}_{t-1}) \geq d$, and $Md_{\emptyset} \geq Md$.

In Appendix B, we investigate the solutions that satisfy (12).

3.4 BER at High SNRs and SNRbs

Here, we consider the case $Md_{\emptyset} \geq Md$. Taking into account that $\mathrm{P}_{\mathrm{X^P}} \approx \mathrm{P}_{\mathrm{X^P|O}}$ and noting (10), we can derive:

$$\mathrm{P}_{\mathrm{X^P}}(SNR_{\mathrm{X^P}} = u_{\mathrm{X^P}}) \approx L^{-1} \sum_{l=1}^{L} (B_{\mathrm{X}} \mathrm{P}_{\mathrm{X}}(SNR_{\mathrm{X}} = u_l) / B_{\mathrm{X^P}}). \tag{13}$$

Using $SNRb = SNR / \bar{B}$, the SNRbs of $\mathbf{X}_t^{\mathrm{P}}$ and equivalent $\mathbf{X}_t$ can be written as follows:

$$v_{\mathrm{X^P}} = u_{\mathrm{X^P}} / \bar{B}_{\mathrm{X^P}} = \mathrm{E}_c \, \mathrm{E}_{\mathbf{X}} / B_{\mathrm{X^P}} \tag{14}$$

and

$$v_l = u_l / \bar{B}_{\mathrm{X}} = 2\sigma_l \, \mathrm{E}_{\mathrm{X}} / B_{\mathrm{X}}, \tag{15}$$

respectively. Note that the $SNRb$ of $\mathbf{X}_t$ in (3) is

$$v_{\mathrm{X}} = u_{\mathrm{X}} / \bar{B}_{\mathrm{X}} = \mathrm{E}_{\mathrm{X}} / B_{\mathrm{X}}. \tag{16}$$

Considering (14), (15), and (16), we arrive at:

$$\mathrm{P}_{\mathrm{X^P}}(SNRb_{\mathrm{X^P}} = u_{\mathrm{X^P}} / \bar{B}_{\mathrm{X^P}}) = \mathrm{P}_{\mathrm{X^P}}(SNR_{\mathrm{X^P}} = u_{\mathrm{X^P}}), \tag{17}$$

$$\mathrm{P}_{\mathrm{X}}(SNRb_{\mathrm{X}} = u_l / \bar{B}_{\mathrm{X}}) = \mathrm{P}_{\mathrm{X}}(SNR_{\mathrm{X}} = u_l), \tag{18}$$

and

$$\mathrm{P}_{\mathrm{X}}(SNRb_{\mathrm{X}} = u_{\mathrm{X}} / \bar{B}_{\mathrm{X}}) = \mathrm{P}_{\mathrm{X}}(SNR_{\mathrm{X}} = u_{\mathrm{X}}). \tag{19}$$

Moreover, with reference to (13) we have

$$\begin{aligned} \mathrm{P}_{\mathrm{X^P}}(SNRb_{\mathrm{X^P}} = u_{\mathrm{X^P}} / \bar{B}_{\mathrm{X^P}}) &= \mathrm{P}_{\mathrm{X^P}}(SNR_{\mathrm{X^P}} = u_{\mathrm{X^P}}) \\ &\approx L^{-1} \sum_{l=1}^{L} (B_{\mathrm{X}} \mathrm{P}_{\mathrm{X}}(SNR_{\mathrm{X}} = u_l) / B_{\mathrm{X^P}}) \\ &= L^{-1} \sum_{l=1}^{L} (B_{\mathrm{X}} \mathrm{P}_{\mathrm{X}}(SNRb_{\mathrm{X}} = u_l / \bar{B}_{\mathrm{X}}) / B_{\mathrm{X^P}}). \end{aligned} \tag{20}$$

At high SNRs, $\mathrm{P}_{\mathrm{X}} = \kappa_{\mathrm{X}} SNR^{-d_{\mathrm{X}} M}$, where κ_{X} is a positive constant independent of SNR [19]. As a result,

$$\mathrm{P}_{\mathrm{X}}(SNR_{\mathrm{X}} = u_{\mathrm{X}}) \approx \kappa_{\mathrm{X}} \, u_{\mathrm{X}}^{-d_{\mathrm{X}} M}, \tag{21}$$

$$\mathrm{P}_{\mathrm{X}}(SNR_{\mathrm{X}} = u_l) \approx \kappa_{\mathrm{X}} \, u_l^{-d_{\mathrm{X}} M}. \tag{22}$$

From (13) and (22), we have

$$\mathrm{P}_{\mathrm{X^P}}(SNR_{\mathrm{X^P}} = u_{\mathrm{X^P}}) \approx (B_{\mathrm{X}} / B_{\mathrm{X^P}}) \kappa_{\mathrm{X}} (L^{-1} \sum_{l=1}^{L} u_l^{-d_{\mathrm{X}} M}). \tag{23}$$

Using $u_l = 2\sigma_l \mathrm{E}_{\mathrm{X}} / N$ and $u_{\mathrm{X^P}} = \mathrm{E}_c \mathrm{E}_{\mathrm{X}} / (N+1)$, we can obtain $u_l = (2\sigma_l / \mathrm{E}_c)((N+1)/N) u_{\mathrm{X^P}}$. So,

$$\mathrm{P}_{\mathrm{X^P}}(SNR_{\mathrm{X^P}} = u_{\mathrm{X^P}}) \approx \kappa_{\mathrm{X^P}} \, u_{\mathrm{X^P}}^{-d_{\mathrm{X}} M} \tag{24}$$

where

$$\kappa_{\mathrm{X^P}} = (B_{\mathrm{X}} / B_{\mathrm{X^P}}) \kappa_{\mathrm{X}} (N / (N+1))^{d_{\mathrm{X}} M} \eta \tag{25}$$

and

$$\eta = L^{-1} \sum_{l=1}^{L} (2\sigma_l / \mathrm{E}_c)^{-d_{\mathrm{X}} M}. \tag{26}$$

Noting (14), (17), and (24), we can deduce:

$$\begin{aligned} \mathrm{P}_{\mathrm{X^P}}(SNRb_{\mathrm{X^P}} = u_{\mathrm{X^P}} / \bar{B}_{\mathrm{X^P}}) &= \mathrm{P}_{\mathrm{X^P}}(SNR_{\mathrm{X^P}} = u_{\mathrm{X^P}}) \\ &\approx \kappa_{\mathrm{X^P}} \, u_{\mathrm{X^P}}^{-d_{\mathrm{X}} M} \\ &= \kappa_{\mathrm{X^P}} \, \bar{B}_{\mathrm{X^P}}^{-d_{\mathrm{X}} M} \, v_{\mathrm{X^P}}^{-d_{\mathrm{X}} M}. \end{aligned} \tag{27}$$

Consequently, from (14), we have

$$\mathrm{P}_{\mathrm{X^P}}(SNRb_{\mathrm{X^P}} = v_{\mathrm{X^P}}) \approx \vartheta_{\mathrm{X^P}} \, v_{\mathrm{X^P}}^{-d_{\mathrm{X}} M} \tag{28}$$

where $\vartheta_{\mathrm{X^P}} = \kappa_{\mathrm{X^P}} \bar{B}_{\mathrm{X^P}}^{-d_{\mathrm{X}} M}$.

Similarly, by using (16), (19), and (21), the BER can be expressed as:

$$\begin{aligned} \mathrm{P}_{\mathrm{X}}(SNRb_{\mathrm{X}} = u_{\mathrm{X}} / \bar{B}_{\mathrm{X}}) &= \mathrm{P}_{\mathrm{X}}(SNR_{\mathrm{X}} = u_{\mathrm{X}}) \\ &\approx \kappa_{\mathrm{X}} \, u_{\mathrm{X}}^{-d_{\mathrm{X}} M} \\ &= \kappa_{\mathrm{X}} \, \bar{B}_{\mathrm{X}}^{-d_{\mathrm{X}} M} \, v_{\mathrm{X}}^{-d_{\mathrm{X}} M}. \end{aligned} \tag{29}$$

Therefore, considering (16) we have

$$\mathrm{P}_{\mathrm{X}}(SNRb_{\mathrm{X}} = v_{\mathrm{X}}) \approx \vartheta_{\mathrm{X}} \, v_{\mathrm{X}}^{-d_{\mathrm{X}} M} \tag{30}$$

where $\vartheta_{\mathrm{X}} = \kappa_{\mathrm{X}} \bar{B}_{\mathrm{X}}^{-d_{\mathrm{X}} M}$.

Considering (25), we obtain

$$\kappa_{\mathrm{X^P}} / \kappa_{\mathrm{X}} = (B_{\mathrm{X}} / B_{\mathrm{X^P}})(N / (N+1))^{d_{\mathrm{X}} M} \eta \tag{31}$$

and

$$\begin{aligned} \vartheta_{\mathrm{X^P}} / \vartheta_{\mathrm{X}} &= (\kappa_{\mathrm{X^P}} / \kappa_{\mathrm{X}})(\bar{B}_{\mathrm{X^P}} / \bar{B}_{\mathrm{X}})^{-d_{\mathrm{X}} M} \\ &= (B_{\mathrm{X}} / B_{\mathrm{X^P}})^{(d_{\mathrm{X}} M + 1)} \eta. \end{aligned} \tag{32}$$

For the case $\eta \approx 1$, we have

$$\kappa_{\mathrm{X^P}} / \kappa_{\mathrm{X}} \approx (B_{\mathrm{X}} / B_{\mathrm{X^P}})(N / (N+1))^{d_{\mathrm{X}} M} \tag{33}$$

and

$$\vartheta_{\mathrm{X^P}} / \vartheta_{\mathrm{X}} \approx (B_{\mathrm{X}} / B_{\mathrm{X^P}})^{(d_{\mathrm{X}} M + 1)}. \tag{34}$$

Thus, noting $B_{\mathrm{X}} < B_{\mathrm{X^P}}$ and $N < N+1$, it is concluded that $\kappa_{\mathrm{X^P}} / \kappa_{\mathrm{X}}$ and $\vartheta_{\mathrm{X^P}} / \vartheta_{\mathrm{X}}$ decay with M and d_{X}.

As a special case of (13) and (20), when the absolute value of c_t is constant ($|c_l| = |c_{t-1}| = c$ for all o_ts and ts), then $\sigma_l = 0.5$ and $u_l = \mathrm{E_X} / N$ for $l = 1,\ldots,L$. Therefore,

$$\begin{aligned} \mathrm{P}_{\mathrm{X^P}}(SNR_{\mathrm{X^P}} &= \mathrm{E_X}/(N+1)) \\ &\approx B_{\mathrm{X}} / B_{\mathrm{X^P}}\, \mathrm{P_X}(SNR_{\mathrm{X}} = \mathrm{E_X}/N) \end{aligned} \tag{35}$$

and

$$\begin{aligned} \mathrm{P}_{\mathrm{X^P}}(SNRb_{\mathrm{X^P}} &= \mathrm{E_X}/B_{\mathrm{X^P}}) \\ &\approx B_{\mathrm{X}} / B_{\mathrm{X^P}}\, \mathrm{P_X}(SNRb_{\mathrm{X}} = \mathrm{E_X}/B_{\mathrm{X}}). \end{aligned} \tag{36}$$

Considering (35), (36), and the fact that $B_{\mathrm{X}} < B_{\mathrm{X^P}}$, we conclude that despite the lower SNR and SNRb ($\mathrm{E_X}/(N+1) < \mathrm{E_X}/N$ and $\mathrm{E_X}/B_{\mathrm{X^P}} < \mathrm{E_X}/B_{\mathrm{X}}$), $\mathbf{X}_t^{\mathrm{P}}$ achieves a lower BER than $\mathbf{X}_t$.

4. Results

Different DSM schemes were simulated to gain a clear understanding of the error performance of the proposed scheme. We assess the performance of the proposed scheme and compare it with CDSM and GCO (GCO schemes in [10] have structures similar to CDSM, and we can design new schemes by employing them). The number of receive antennas is set to 1 ($M = 1$) for simplicity. The appropriate values of c_t were chosen using a computer search. It is worth mentioning that in the simulation of a BER of 10^{-m}, according to [21], a minimum of 10^{m+3} channel realizations were used.

CDSM and the proposed scheme: Tables 2 and 3 provide the characteristics of the proposed scheme and CDSM. For clarification, the structure of the proposed scheme $\mathbf{X}_t^{\mathrm{P}}$ is presented in Tab. 4 ($N = 3$, 4-PSK). For simplicity, in the simulations, the non-zero elements of $\mathbf{A}_t$ are set to 1. Figures 1, 2, 3, and 4 illustrate the BER performance for two and three transmit antennas. In the case that the proposed scheme has higher throughput (2 versus 1.5 bpcu), it achieves either the same or less BER than CDSM. Additionally, for approximately the same throughputs (1.33 versus 1.5, 1.75 versus 1.66, and 2.5 versus 2.66 bpcu), the proposed scheme yields a significantly lower BER than CDSM. Furthermore, it is observed that analytical evaluations are validated by simulation results at high SNRs and SNRbs (formulas are not applicable for low SNRs). The required SNRs and SNRbs to achieve a BER of 5×10^{-4} are presented in Tab. 3. The results indicate the efficiency of the proposed scheme.

GCO and the proposed scheme: Tables 5 and 6 show the characteristics of the proposed scheme and GCO. In Figs. 5 and 6, GCO in [10] and the proposed scheme have 4 transmit antennas ($N = 4$). The indices $o_t = 1,2,3$, and 4 are sufficient to create the new index bits (2 bits) of the proposed scheme ($o_t = 5$ is not used). The proposed scheme has 6 index bits, whereas the employed GCO has 4 index bits. Antenna index permutations of these 4 bits are selected according to GCO requirements. According to GCO, each index bit sequence has only one difference from adjacent index bit sequence. Also, there are only two antennas indices difference between two adjacent antenna index permutations. The BER performances of the proposed scheme and GCO are compared under the same spectral efficiency of 2 bpcu. In the codes with transmit diversity order of 2, two 4-PSK symbols are employed ($\mathbf{s}_t = [s_1, s_1, s_2, s_2]$). The results show that the proposed scheme achieves lower BER.

$N = 2$	2-PSK		$o_t = 1$	$o_t = 2$		
		Odd t	$1\angle 0°$	$1\angle 55°$		
		Even t	$1\angle 0°$	$1\angle 135°$		
	4-PSK		$o_t = 1$	$o_t = 2$		
		Odd t	$1\angle 66°$	$1\angle 110°$		
		Even t	$1\angle 78°$	$1\angle 130°$		
$N = 3$	2-PSK		$o_t = 1$	$o_t = 2$	$o_t = 3$	$o_t = 4$
		Odd t	$1\angle 0°$	$1\angle 41.4°$	$1\angle 82.8°$	$1\angle 124.2°$
		Even t	$1\angle 0°$	$1\angle 52.2°$	$1\angle 104.4°$	$1\angle 156.6°$
	4-PSK		$o_t = 1$	$o_t = 2$	$o_t = 3$	$o_t = 4$
		Odd t	$1\angle 23.4°$	$1\angle -23.4°$	$1\angle 46.8°$	$1\angle -46.8°$
		Even t	$1\angle 12.6°$	$1\angle -12.6°$	$1\angle 25.2°$	$1\angle -25.2°$

Tab. 2. Values of c_t in simulation of the proposed $\mathbf{X}_t^{\mathrm{P}}$ for $N = 2, 3$.

Number of transmit antennas	$N = 2$			$N = 3$			
Scheme	$\mathbf{X}_t$	$\mathbf{X}_t^{\mathrm{P}}$	$\mathbf{X}_t^{\mathrm{P}}$	$\mathbf{X}_t$	$\mathbf{X}_t^{\mathrm{P}}$	$\mathbf{X}_t$	$\mathbf{X}_t^{\mathrm{P}}$
Number of time slots	2	3	3	3	4	3	4
PSK size	2	2	4	2	2	4	4
Number of symbols	2	2	2	3	3	3	3
Total index bits	1	1+1	1+1	2	2+2	2	2+2
Rank of $\mathbf{D}_t$ for $\varnothing$	-	2	2	-	3	-	3
Diversity order	1	1	1	1	1	1	1
Throughput (bpcu)	1.5	1.33	2	1.66	1.75	2.66	2.5
κ in $\mathrm{P} = \kappa SNR^{-1}$	1	0.54	1	0.99	0.53	2.21	1.4
ϑ in $\mathrm{P} = \vartheta SNRb^{-1}$	0.67	0.37	0.51	0.94	0.49	2	1.24
SNR (dB) for BER = 5×10^{-4}	33	30	33	33	31	37	34
SNRb (dB) for BER = 5×10^{-4}	31	28.5	30.5	31	28	37.2	30

Tab. 3. Characteristics of schemes $\mathbf{X}_t$ (CDSM) and $\mathbf{X}_t^{\mathrm{P}}$ (proposed).

	Odd block times t	Even block times t
$o_t = 1$	$1\angle 23.4° \times \begin{bmatrix} 0 & 0 & 0 \\ \mathbf{X}_t(1,:) \\ \mathbf{X}_t(2,:) \\ \mathbf{X}_t(3,:) \end{bmatrix}$	$1\angle 12.6° \times \begin{bmatrix} 0 & 0 & 0 \\ \mathbf{X}_t(1,:) \\ \mathbf{X}_t(2,:) \\ \mathbf{X}_t(3,:) \end{bmatrix}$
$o_t = 2$	$1\angle -23.4° \times \begin{bmatrix} \mathbf{X}_t(3,:) \\ 0 & 0 & 0 \\ \mathbf{X}_t(1,:) \\ \mathbf{X}_t(2,:) \end{bmatrix}$	$1\angle -12.6° \times \begin{bmatrix} \mathbf{X}_t(3,:) \\ 0 & 0 & 0 \\ \mathbf{X}_t(1,:) \\ \mathbf{X}_t(2,:) \end{bmatrix}$
$o_t = 3$	$1\angle 46.8° \times \begin{bmatrix} \mathbf{X}_t(2,:) \\ \mathbf{X}_t(3,:) \\ 0 & 0 & 0 \\ \mathbf{X}_t(1,:) \end{bmatrix}$	$1\angle 25.2° \times \begin{bmatrix} \mathbf{X}_t(2,:) \\ \mathbf{X}_t(3,:) \\ 0 & 0 & 0 \\ \mathbf{X}_t(1,:) \end{bmatrix}$
$o_t = 4$	$1\angle -46.8° \times \begin{bmatrix} \mathbf{X}_t(1,:) \\ \mathbf{X}_t(2,:) \\ \mathbf{X}_t(3,:) \\ 0 & 0 & 0 \end{bmatrix}$	$1\angle -25.2° \times \begin{bmatrix} \mathbf{X}_t(1,:) \\ \mathbf{X}_t(2,:) \\ \mathbf{X}_t(3,:) \\ 0 & 0 & 0 \end{bmatrix}$

Tab. 4. Transmit signal matrices of the proposed $\mathbf{X}_t^{\mathrm{P}}$ for $N = 3$ and 4-PSK.

			$o_t = 1$	$o_t = 2$	$o_t = 3$	$o_t = 4$
$N = 4$	2-PSK	Odd t	$1\angle 0°$	$1\angle 41.4°$	$1\angle 82.8°$	$1\angle 124.2°$
		Even t	$1\angle 0°$	$1\angle 52.2°$	$1\angle 104.4°$	$1\angle 156.6°$
			$o_t = 1$	$o_t = 2$	$o_t = 3$	$o_t = 4$
	4-PSK	Odd t	$1\angle 0°$	$1\angle -19.8°$	$1\angle 46.8°$	$1\angle -39.6°$
		Even t	$1\angle 30.6°$	$1\angle 16.2°$	$1\angle 61.2°$	$1\angle 0°$

Tab. 5. Values of c_t in simulation of the proposed $\mathbf{X}_t^{\mathrm{P}}$ for $N = 4$.

No. of transmit antennas	$N = 4$		$N = 4$	
Scheme	$\mathbf{X}_t$	$\mathbf{X}_t^{\mathrm{P}}$	$\mathbf{X}_t$	$\mathbf{X}_t^{\mathrm{P}}$
No. of time slots	4	5	4	5
PSK size	2	2	4	4
No. of symbols	4	4	2	2
Total index bits	4	4+2	4	4+2
Rank of $\mathbf{D}_t$ for Ø	-	2	-	3
Diversity order	1	1	2	2
Throughput (bpcu)	2	2	2	2
Index bits of the GCO	$q_{t,i}$ (nonzero coefficient of the i-th column of $\mathbf{A}_t$)			
0000	$q_{t,1}, q_{t,2}, q_{t,3}, q_{t,4} = 1$		$q_{t,1}, q_{t,2} = 1, q_{t,3}, q_{t,4} = e^{j\pi/24}$	
0001	$q_{t,1}, q_{t,2}, q_{t,3}, q_{t,4} = 1$		$q_{t,1}, q_{t,2} = 1, q_{t,3}, q_{t,4} = e^{j2\pi/24}$	
⋮	⋮		⋮	
1110	$q_{t,1}, q_{t,2}, q_{t,3}, q_{t,4} = 1$		$q_{t,1}, q_{t,2} = 1, q_{t,3}, q_{t,4} = e^{j15\pi/24}$	
1111	$q_{t,1}, q_{t,2}, q_{t,3}, q_{t,4} = 1$		$q_{t,1}, q_{t,2} = 1, q_{t,3}, q_{t,4} = e^{j16\pi/24}$	
κ	1.62	1.05	31.8	18.5
ϑ	0.82	0.52	8.1	4.63
SNR (dB) for $BER = 2 \times 10^{-4}$	39.19	37.17	25.75	25.38
SNR (dB) for $BER = 2 \times 10^{-6}$	-	-	36.06	34.83
SNRb (dB) for $BER = 2 \times 10^{-4}$	36.16	34.15	22.74	22.36
SNRb (dB) for $BER = 5 \times 10^{-6}$	-	-	33.04	31.81

Tab. 6. Characteristics of schemes $\mathbf{X}_t$ (GCO) and $\mathbf{X}_t^{\mathrm{P}}$ (proposed).

From Figs. 1, 2, 3, 4, 5, and 6, it is observed that the proposed scheme with new index bits, maintains the same transmit diversity order as those of the employed CDSM and GCO.

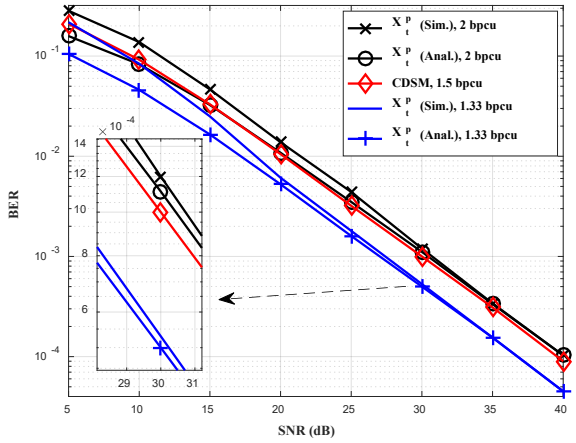

Fig. 1. BER vs SNR of the proposed scheme and CDSM for $N = 2$.

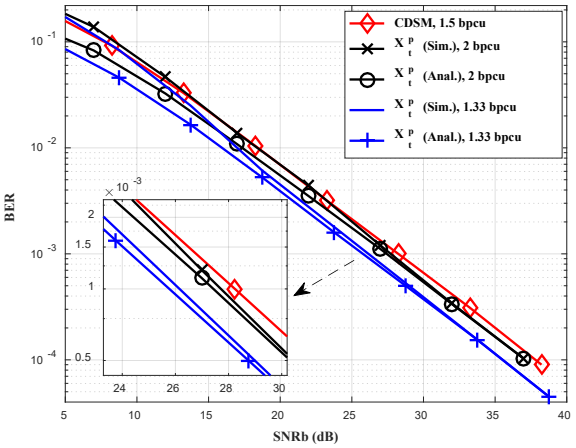

Fig. 2. BER vs SNRb of the proposed scheme and CDSM for $N = 2$.

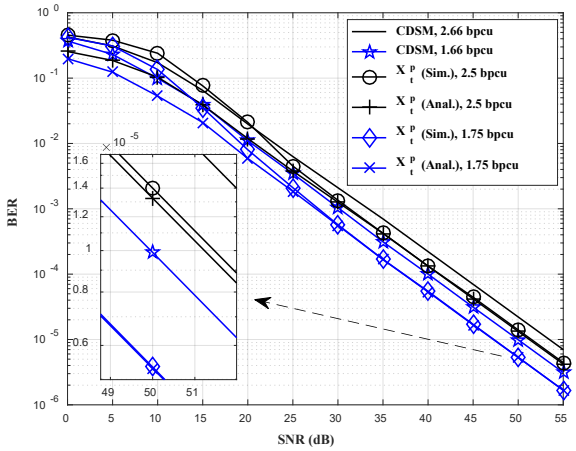

Fig. 3. BER vs SNR of the proposed scheme and CDSM for $N = 3$.

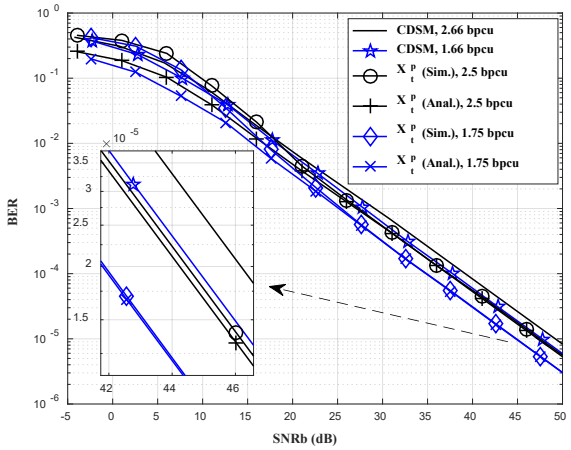

Fig. 4. BER vs SNRb of the proposed scheme and CDSM for $N = 3$.

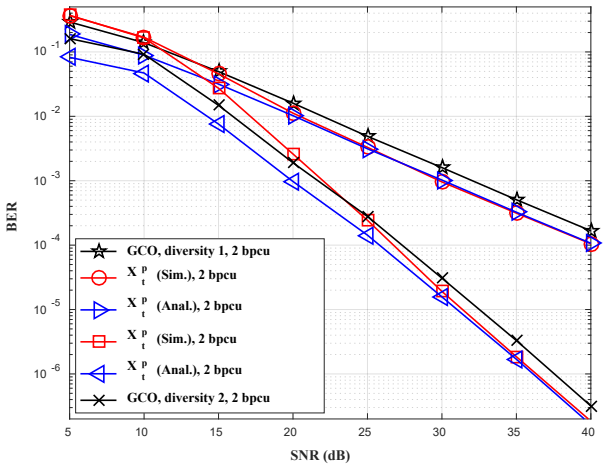

Fig. 5. BER vs SNR of the proposed scheme and GCO [10] for $N = 4$.

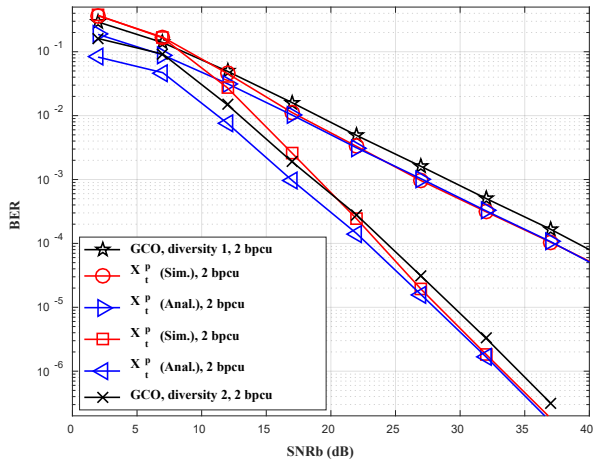

Fig. 6. BER vs SNRb of the proposed scheme and GCO [10] for $N = 4$.

5. Conclusion

In this study, we proposed a new scheme that includes an empty time slot and time slots of a CDSM (or GCO). The introduced detector avoids error propagation. The proposed scheme achieves the same diversity order as those of the utilized CDSM and GCO. The obtained expressions for error probability can be used to investigate the impacts of the number of new index bits, values of coefficients, etc., on the performance of the proposed scheme. Simulation results confirmed theoretical discussions and showed the efficiency of the presented scheme.

References

[1] MANDLOI, M., GURJAR, D., PATTANAYAK, P., et al. *5G and Beyond Wireless Systems.* Springer, 2021. DOI: 10.1007/978-981-15-6390-4

[2] CHENG, X., ZHANG, M., WEN, M., et al. Index modulation for 5G: Striving to do more with less. *IEEE Wireless Communications,* 2018, vol. 25, no. 2, p. 126–132. DOI: 10.1109/MWC.2018.1600355

[3] TUSHA, S. D., TUSHA, A., BASAR, E., et al. Multidimensional index modulation for 5G and beyond wireless networks. *Proceedings of the IEEE,* 2020, vol. 109, no. 2, p. 170–199. DOI: 10.1109/JPROC.2020.3040589

[4] FAZELI, A., NGUYEN, H. H., TUAN, H. D., et al. Non-coherent multi-level index modulation. *IEEE Transactions on Communications,* 2022, vol. 70, no. 4, p. 2240–2255. DOI: 10.1109/TCOMM.2022.3142159

[5] JOSE, D., SAMEER, S. Differential transmission schemes for generalized spatial modulation. *IEEE Transactions on Vehicular Technology,* 2021, vol. 70, no. 12, p. 12640–12650. DOI: 10.1109/TVT.2021.3118457

[6] ZOU, H., QUAN, D., JIN, X., et al. Differential space time media-based modulation system. *IET Communications,* 2022, vol. 16, no. 9, p. 942–950. DOI: 10.1049/cmu2.12396

[7] ISHIKAWA, N., SUGIURA, S. Unified differential spatial modulation. *IEEE Wireless Communications Letters,* 2014, vol. 3, no. 4, p. 337–340. DOI: 10.1109/LWC.2014.2315635

[8] DWARIKA, K., XU, H. Differential full diversity spatial modulation using amplitude phase shift keying. *Radioengineering,* 2018, vol. 27, no. 1, p. 151–158. DOI: 10.13164/re.2018.0151

[9] DWARIKA, K., XU, H. Power allocation and low complexity detector for differential full diversity spatial modulation using two transmit antennas. *Radioengineering,* 2017, vol. 26, no. 2, p. 461 to 469. DOI: 10.13164/re.2017.0461

[10] LI, J., WEN, M., CHENG, X., et al. Differential spatial modulation with Gray coded antenna activation order. *IEEE Communications Letters,* 2016, vol. 20, no. 6, p. 1100–1103. DOI: 10.1109/LCOMM.2016.2557801

[11] XIAO, L., XIAO, Y., YANG, J., et al. Space-time block coded differential spatial modulation. *IEEE Transactions on Vehicular Technology,* 2017, vol. 66, no. 10, p. 8821–8834. DOI: 10.1109/TVT.2017.2696380

[12] XIAO, L., CHEN, D., HEMADEH, I. A., et al. Graph theory assisted bit-to-index-combination Gray coding for generalized index modulation. *IEEE Transactions on Wireless Communications,* 2020, vol. 19, no. 12, p. 8232–8245. DOI: 10.1109/TWC.2020.3020692

[13] BIAN, Y., CHENG, X., WEN, M., et al. Differential spatial modulation. *IEEE Transactions on Vehicular Technology,* 2015, vol. 64, no. 7, p. 3262–3268. DOI: 10.1109/TVT.2014.2348791

[14] MARTIN, P. A. Differential spatial modulation for APSK in time-varying fading channels. *IEEE Communications Letters,* 2015, vol. 19, no. 7, p. 1261–1264. DOI: 10.1109/LCOMM.2015.2426172

[15] LIU, J., DAN, L., YANG, P., et al. High-rate APSK-aided differential spatial modulation: Design method and performance analysis. *IEEE Communications Letters,* 2016, vol. 21, no. 1, p. 168–171. DOI: 10.1109/LCOMM.2016.2610962

[16] ISHIKAWA, N., SUGIURA, S. Rectangular differential spatial modulation for open-loop noncoherent massive-MIMO downlink. *IEEE Transactions on Wireless Communications,* 2017, vol. 16, no. 3, p. 1908–1920. DOI: 10.1109/TWC.2017.2657497

[17] XIAO, L., XIAO, P., RUAN, H., et al. Differentially-encoded rectangular spatial modulation approaches the performance of its coherent counterpart. *IEEE Transactions on Communications,* 2020, vol. 68, no. 12, p. 7593–7607. DOI: 10.1109/TCOMM.2020.3021117

[18] WEI, R. Y., CHANG, C. W. A low-complexity soft-output detector for differential spatial modulation. *IEEE Wireless Communications Letters,* 2022, vol. 11, no. 5, p. 1077–1081. DOI: 10.1109/LWC.2022.3156889

[19] PROAKIS, J. G., SALEHI, M. *Digital Communications*. 5th ed. McGraw-Hill, Education, 2007. ISBN: 9780072957167

[20] HORN, R. A., JOHNSON, C. R. *Matrix Analysis*. Cambridge University Press, 1985. DOI: 10.1017/CBO9780511810817

[21] LOYKA, S., GAGNON, F. On accuracy and efficiency of Monte-Carlo BER simulations for fading channel. In *2007 International Symposium on Signals, Systems and Electronics.* Montreal (Canada), 2007, p. 255–258. DOI: 10.1109/ISSSE.2007.4294461

About the Authors ...

Vahid ABBASI (corresponding author) received the B.S degree in Electrical Engineering from Azarbaijan Shahid Madani University, Tabriz, Iran, in 2012, and the M.S. degree in Electrical Engineering from Urmia University, Urmia, Iran, in 2015. He is currently a candidate of Ph.D. degree in Electrical Engineering at Urmia University, Urmia, Iran. His research interests include MIMO communication systems, index modulation and signal processing.

Mahrokh G. SHAYESTEH received the B.Sc. degree from the University of Tehran, Tehran, Iran; the M.Sc. degree from Khajeh Nassir University of Technology, Tehran, Iran; and the Ph.D. degree from Amir Kabir University of Technology, Tehran, Iran, all in Electrical Engineering. She is currently with the Department of Electrical Engineering, Urmia University, Urmia, Iran, and also working with the Wireless Research Laboratory, Advanced Communication Research Institute (ACRI), Department of Electrical Engineering, Sharif University of Technology, Tehran, Iran. Her research interests include wireless communications, signal and image processing.

Appendix A: Diversity Order of Ø

Considering the structure of $\mathbf{C}_t$ and $\mathbf{S}_t$, all columns of $\mathbf{F}_t$ have exactly one non-zero element. Additionally, the o_t-th row of $\mathbf{F}_t$ is zero. Noting the structure of $\tilde{\mathbf{C}}^{\mathrm{T}}_{t-1}$ and $\mathbf{C}_{t-1}$, the maximum number of non-zero elements in each row and each column of $\tilde{\mathbf{C}}^{\mathrm{T}}_{t-1}\mathbf{C}_{t-1}$ is 1. Thus, the maximum number of non-zero elements in each row and each column of $\tilde{\mathbf{S}}_t\tilde{\mathbf{C}}^{\mathrm{T}}_{t-1}\tilde{c}^{-1}_{t-1}c_{t-1}\mathbf{C}_{t-1}$ is 1. Therefore, the maximum number of non-zero elements in each row and column of $\mathbf{Q}_t = \tilde{c}_t\tilde{\mathbf{C}}_t\tilde{\mathbf{S}}_t\tilde{\mathbf{C}}^{\mathrm{T}}_{t-1}\tilde{c}^{-1}_{t-1}c_{t-1}\mathbf{C}_{t-1}$ is 1. Furthermore, as the $\tilde{o}_t$-th row of $\tilde{c}_t\tilde{\mathbf{C}}_t$ is empty, the $\tilde{o}_t$-th row of $\mathbf{Q}_t$ is a zero vector. We show the non-zero element of the n-th column of $\mathbf{C}_t\mathbf{S}_t$ by s_n. In this way, if the n-th column of $\tilde{\mathbf{C}}_t\tilde{\mathbf{S}}_t\tilde{\mathbf{C}}^{\mathrm{T}}_{t-1}\mathbf{C}_{t-1}$ has a non-zero element, $\tilde{s}_n$ denotes it. a_n and $\tilde{a}_n$ are the coefficients of used symbols in s_n and $\tilde{s}_n$, respectively. As an example, for the case

$$\mathbf{C}_{t-1}=\begin{bmatrix}0&0&1\\0&0&0\\1&0&0\\0&1&0\end{bmatrix},\qquad \tilde{\mathbf{C}}_{t-1}=\begin{bmatrix}0&1&0\\0&0&1\\0&0&0\\1&0&0\end{bmatrix},$$

$$\mathbf{C}_{t}=\begin{bmatrix}1&0&0\\0&1&0\\0&0&1\\0&0&0\end{bmatrix},\qquad \tilde{\mathbf{C}}_{t}=\begin{bmatrix}0&0&0\\1&0&0\\0&1&0\\0&0&1\end{bmatrix},$$

$$\tilde{\mathbf{S}}_t=\begin{bmatrix}0&\tilde{s}_2&0\\0&0&\tilde{s}_3\\\tilde{s}_1&0&0\end{bmatrix},\ \text{and}\ \mathbf{S}_t=\begin{bmatrix}0&s_2&0\\s_1&0&0\\0&0&s_3\end{bmatrix},$$

we have

$$\tilde{\mathbf{C}}^{\mathrm{T}}_{t-1}\mathbf{C}_{t-1}=\begin{bmatrix}0&1&0\\0&0&1\\0&0&0\end{bmatrix},\ \tilde{\mathbf{S}}_t\tilde{\mathbf{C}}^{\mathrm{T}}_{t-1}\mathbf{C}_{t-1}=\begin{bmatrix}0&0&\tilde{s}_2\\0&0&0\\0&\tilde{s}_1&0\end{bmatrix},$$

$$\tilde{\mathbf{C}}_t\tilde{\mathbf{S}}_t\tilde{\mathbf{C}}^{\mathrm{T}}_{t-1}\mathbf{C}_{t-1}=\begin{bmatrix}0&0&0\\0&0&\tilde{s}_2\\0&0&0\\0&\tilde{s}_1&0\end{bmatrix},$$

and

$$\mathbf{C}_t\mathbf{S}_t=\begin{bmatrix}0&s_2&0\\s_1&0&0\\0&0&s_3\\0&0&0\end{bmatrix}.$$

As a result,

$$\mathbf{D}_t = c_t \mathbf{C}_t \mathbf{S}_t - \tilde{c}_t \tilde{\mathbf{C}}_t \tilde{\mathbf{S}}_t \tilde{\mathbf{C}}_{t-1}^{\mathrm{T}} \tilde{c}_{t-1}^{-1} c_{t-1} \mathbf{C}_{t-1}$$
$$= c_t \begin{bmatrix} 0 & s_2 & 0 \\ s_1 & 0 & 0 \\ 0 & 0 & s_3 \\ 0 & 0 & 0 \end{bmatrix} - \tilde{c}_t \tilde{c}_{t-1}^{-1} c_{t-1} \begin{bmatrix} 0 & 0 & 0 \\ 0 & 0 & \tilde{s}_2 \\ 0 & 0 & 0 \\ 0 & \tilde{s}_1 & 0 \end{bmatrix}$$
$$= \begin{bmatrix} 0 & c_t s_2 & 0 \\ c_t s_1 & 0 & -\tilde{c}_t \tilde{c}_{t-1}^{-1} c_{t-1} \tilde{s}_2 \\ 0 & 0 & c_t s_3 \\ 0 & -\tilde{c}_t \tilde{c}_{t-1}^{-1} c_{t-1} \tilde{s}_1 & 0 \end{bmatrix}.$$

Assume that some columns of $(N + 1) \times N$ matrix $\mathbf{D}_t$ are not independent. Therefore, a zero vector can be formed as a linear combination of these columns, where the coefficients are not all zero [20]. As an example, we consider the following cases:

1) If only one coefficient is non-zero, we have $\sum_{n=1}^{1} e_{i_n} \mathbf{D}_t(:, i_n) = \mathbf{0}$, where e_{i_1} is non-zero. Using $\mathbf{D}_t = \mathbf{F}_t - \mathbf{Q}_t$, we have $e_{i_1} \mathbf{F}_t(:, i_1) = e_{i_1} \mathbf{Q}_t(:, i_1)$ and $\mathbf{F}_t(:, i_1) = \mathbf{Q}_t(:, i_1)$. So, $c_t s_{i_1} = \tilde{\gamma}_t \tilde{s}_{i_1}$, where $\tilde{\gamma}_t = \tilde{c}_t \tilde{c}_{t-1}^{-1} c_{t-1}$.

2) If only two coefficients are non-zero, we have $\sum_{n=1}^{2} e_{i_n} \mathbf{D}_t(:, i_n) = \mathbf{0}$, where e_{i_1} and e_{i_2} are non-zero. Thus, $\sum_{n=1}^{2} e_{i_n} \mathbf{F}_t(:, i_n) = \sum_{n=1}^{2} e_{i_n} \mathbf{Q}_t(:, i_n)$. Considering the discussions on the number of non-zero elements of $\mathbf{F}_t$ and $\mathbf{Q}_t$, there are two subcases as follows:

(a) $e_{i_1} \mathbf{F}_t(:, i_1) = e_{i_2} \mathbf{Q}_t(:, i_2)$, $e_{i_2} \mathbf{F}_t(:, i_2) = e_{i_1} \mathbf{Q}_t(:, i_1)$ and
(b) $e_{i_1} \mathbf{F}_t(:, i_1) = e_{i_1} \mathbf{Q}_t(:, i_1)$, $e_{i_2} \mathbf{F}_t(:, i_2) = e_{i_2} \mathbf{Q}_t(:, i_2)$.

For subcase (a), we have $e_{i_1} c_t s_{i_1} = e_{i_2} \tilde{\gamma}_t \tilde{s}_{i_2}$ and $e_{i_2} c_t s_{i_2} = e_{i_1} \tilde{\gamma}_t \tilde{s}_{i_1}$, where $\tilde{\gamma}_t = \tilde{c}_t \tilde{c}_{t-1}^{-1} c_{t-1}$. Thus, $e_{i_1} e_{i_2} c_t^2 s_{i_1} s_{i_2} = e_{i_1} e_{i_2} \tilde{\gamma}_t^2 \tilde{s}_{i_1} \tilde{s}_{i_2}$ and we arrive at $c_t^2 s_{i_1} s_{i_2} = \tilde{\gamma}_t^2 \tilde{s}_{i_1} \tilde{s}_{i_2}$. Similarly, for subcase (b) we have $c_t^2 s_{i_1} s_{i_2} = \tilde{\gamma}_t^2 \tilde{s}_{i_1} \tilde{s}_{i_2}$.

3) If only three coefficients are non-zero, we have $\sum_{n=1}^{3} e_{i_n} \mathbf{D}_t(:, i_n) = \mathbf{0}$, where e_{i_1}, e_{i_2}, and e_{i_3} are non-zero. Hence, $\sum_{n=1}^{3} e_{i_n} \mathbf{F}_t(:, i_n) = \sum_{n=1}^{3} e_{i_n} \mathbf{Q}_t(:, i_n)$. Considering the discussions on the number of non-zero elements of $\mathbf{F}_t$ and $\mathbf{Q}_t$, there are several subcases. For the subcase ($e_{i_1} \mathbf{F}_t(:, i_1) = e_{i_2} \mathbf{Q}_t(:, i_2)$, $e_{i_2} \mathbf{F}_t(:, i_2) = e_{i_3} \mathbf{Q}_t(:, i_3)$, and $e_{i_3} \mathbf{F}_t(:, i_3) = e_{i_1} \mathbf{Q}_t(:, i_1)$) we have $e_{i_1} c_t s_{i_1} = e_{i_2} \tilde{\gamma}_t \tilde{s}_{i_2}$, $e_{i_2} c_t s_{i_2} = e_{i_3} \tilde{\gamma}_t \tilde{s}_{i_3}$, and $e_{i_3} c_t s_{i_3} = e_{i_1} \tilde{\gamma}_t \tilde{s}_{i_1}$. So, $e_{i_1} e_{i_2} e_{i_3} c_t^3 s_{i_1} s_{i_2} s_{i_3} = e_{i_1} e_{i_2} e_{i_3} \tilde{\gamma}_t^3 \tilde{s}_{i_1} \tilde{s}_{i_2} \tilde{s}_{i_3}$ and we arrive at $c_t^3 s_{i_1} s_{i_2} s_{i_3} = \tilde{\gamma}_t^3 \tilde{s}_{i_1} \tilde{s}_{i_2} \tilde{s}_{i_3}$. Similarly, for the other subcases we obtain $c_t^3 s_{i_1} s_{i_2} s_{i_3} = \tilde{\gamma}_t^3 \tilde{s}_{i_1} \tilde{s}_{i_2} \tilde{s}_{i_3}$.

Considering the above cases, we conclude that if k coefficients $(e_{i_1}, \ldots, e_{i_k})$ are non-zero, then $s_{i_1} \ldots s_{i_k} c_t^k = \tilde{\gamma}_t^k \tilde{s}_{i_1} \ldots \tilde{s}_{i_k}$.

Noting the above discussions, if we provide

$$s_{i_1} \ldots s_{i_k} c_t^k \neq (\tilde{c}_t \tilde{c}_{t-1}^{-1} c_{t-1})^k \tilde{s}_{i_1} \ldots \tilde{s}_{i_k}, \quad k = 1, \ldots, d, \quad d \leq N \tag{37}$$

for all cases of Ø, all values of $s_{i_1}, \ldots, s_{i_k}$, $\tilde{s}_{i_1}, \ldots, \tilde{s}_{i_k}$, and all distinct values of $i_1, \ldots, i_k$ ($1 \leq i_1, \ldots, i_k \leq N$), we will have $\mathrm{rank}(\mathbf{D}_t) \geq d$, $\mathrm{rank}(\mathbf{D}_t \mathbf{X}_{t-1}) \geq d$, and $Md_{\emptyset} \geq Md$.

Appendix B: Satisfying Condition (12)

Since $|s_n| = |\tilde{s}_n| = 1$, we have $|s_{i_1} \ldots s_{i_k}| = |\tilde{s}_{i_1} \ldots \tilde{s}_{i_k}|$, $k = 1, \ldots, d$ thus, a simple solution to meet (12), is to provide $|c_t / \tilde{c}_t| \neq |c_{t-1} / \tilde{c}_{t-1}|$ for all cases of Ø

For the case that $s_1, \ldots, s_N$ are selected from the same $\mathcal{M}$-PSK constellation, multiplying and dividing several $\mathcal{M}$-PSK constellations result in the same $\mathcal{M}$-PSK constellation, hence (12) is converted to

$$a_{i_1} \ldots a_{i_k} \mathrm{e}^{\mathrm{j}2\pi m/\mathcal{M}} c_t^k \neq (\tilde{c}_t \tilde{c}_{t-1}^{-1} c_{t-1})^k \tilde{a}_{i_1} \ldots \tilde{a}_{i_k}, \quad k = 1, \ldots, d, \quad d \leq N \tag{38}$$

where $m = 1, \ldots, \mathcal{M}$.

For the case $s_{i_1} \ldots s_{i_k} = \tilde{s}_{i_1} \ldots \tilde{s}_{i_k}$, (12) is converted to

$$(c_t / \tilde{c}_t)^k \neq (c_{t-1} / \tilde{c}_{t-1})^k, \quad \forall \ [o'_{t-1}, \hat{o}_t] \neq [o_{t-1}, o_t] \tag{39}$$

($c_t^k \neq (\tilde{c}_t \tilde{c}_{t-1}^{-1} c_{t-1})^k$), where $k = 1, \ldots, d$ and $d \leq N$. Therefore, if we use the same set of values for c_ts and c_{t-1}s, satisfying (39) is impossible. For example, for the case ($\tilde{c}_t = \tilde{c}_{t-1}$, $c_t = c_{t-1}$, $\tilde{c}_t \neq c_t$, $\tilde{c}_{t-1} \neq c_{t-1}$), we have $|c_t / \tilde{c}_t| = |c_{t-1} / \tilde{c}_{t-1}|$. So, we propose to use different values for c_ts at odd and even block times (t) (this is necessary but not sufficient condition).